Supplementary Information

Multidrug Resistance Tumors-Aimed Theranostics on the basis of the Strong Electrostatic Attraction of Resistant Cells with Nanomaterials

Shuwei Liu,[a] Lu Wang,[b] Shuyao Li,[a] Xuya Meng,[b] Bin Sun,[b] Xue Zhang,[a] Lening Zhang,*[a,d] Yi Liu,[a] Min Lin,*[c] Hao Zhang,*[a] and Bai Yang[a]

[a] State Key Laboratory of Supramolecular Structure and Materials, College of Chemistry, Jilin University, Changchun 130012, P. R. China. E-mail: hao_zhang@jlu.edu.cn.

[b] Department of Oral Pathology, School and Hospital of Stomatology, Jilin University, Changchun 130021, P. R. China.

[c] Collaborative Innovation Center for Marine Biomass Fibers, Materials and Textiles of Shandong Province, Institute of Marine Biobased Materials, School of Materials Science and Engineering, Qingdao University, Qingdao 266071, P. R. China. Email: linmin900401@126.com.

[d] Department of Thoracic Surgery, China-Japan Union Hospital, Jilin University, Changchun 130033, P. R. China. Email: 951446482@qq.com.

*To whom correspondence should be addressed and H.Z. proposed and supervised the project. Fax: +86 431 85193423.

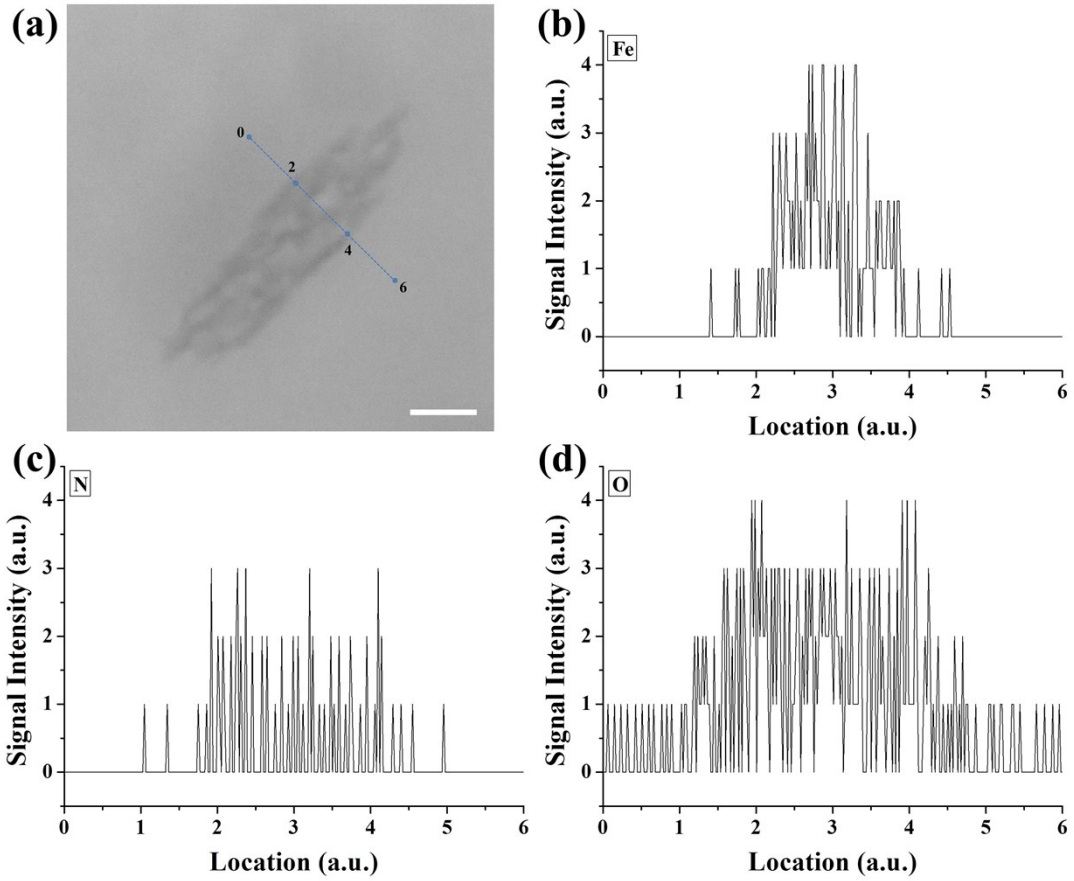

Figure S1. Mapping element line scan of PEG-CuPani NS. (a) TEM image and location information. The scale bar is 10 nm. (b-d) Element distribution of Fe (b), N (c) and O (d).

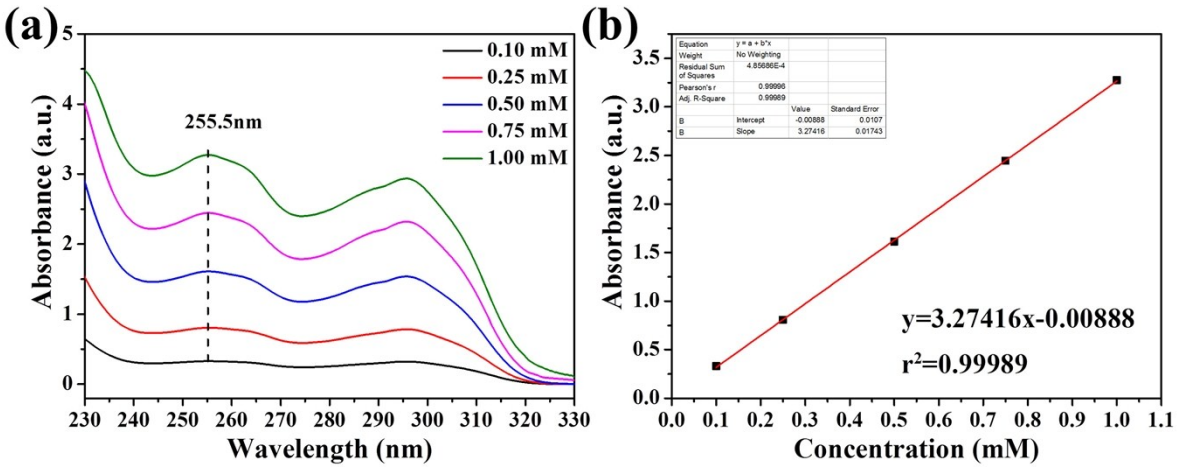

Figure S2. (a) UV-vis absorption spectra of different concentrations of VCR. (b) The standard absorption curve of VCR according to the concentration.

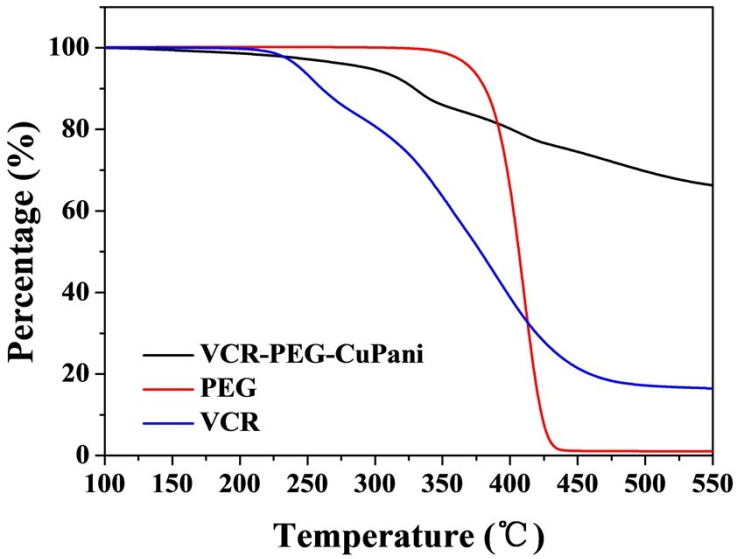

Figure S3. TGA curves of PEG, VCR and VCR-PEG-CuPani NSs.

Table S1. Zeta potential of KB cells, KBV cells, Hela cells, CuPani NSs, and VCR-PEG-CuPani NSs.

	Zeta Potential
KB Cells	**- 23.4 mV**
KBV Cells	**- 29.3 mV**
HeLa Cells	**- 29.1 mV**
CuPani	**+ 33.0 mV**
VCR-PEG-CuPani	**+ 30.3 mV**

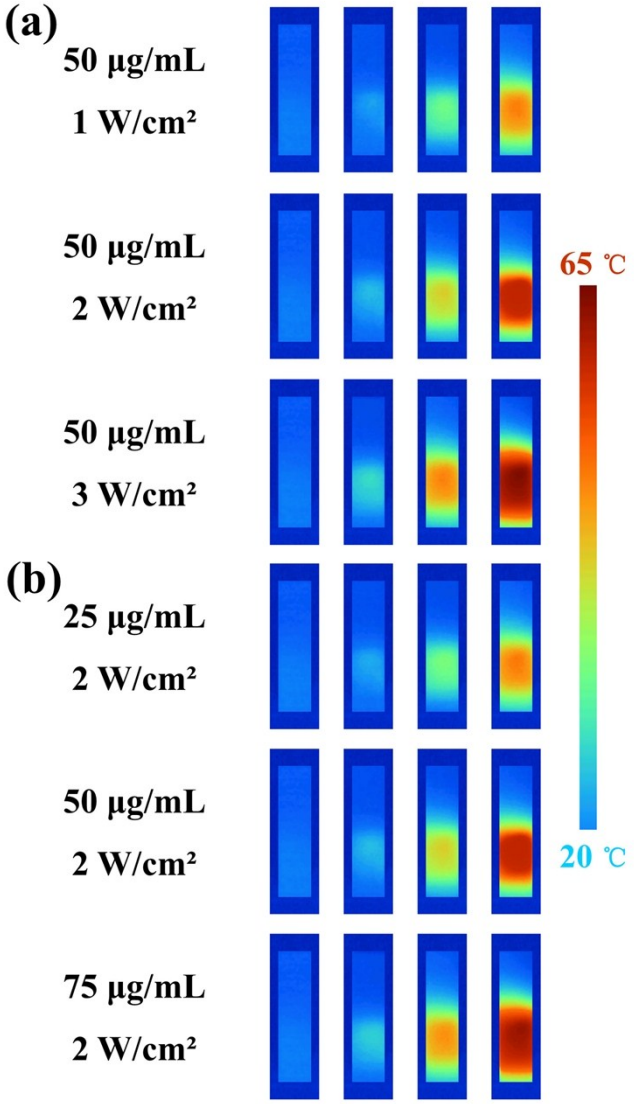

Figure S4. (a) IR thermal images of 50 μg/mL VCR-PEG-CuPani aqueous solution under the irradiation of an 808 nm laser at different power density. (b) IR thermal images of VCR-PEG-CuPani aqueous solution at different concentration under the irradiation of an 808 nm laser at 2 W/cm^2.

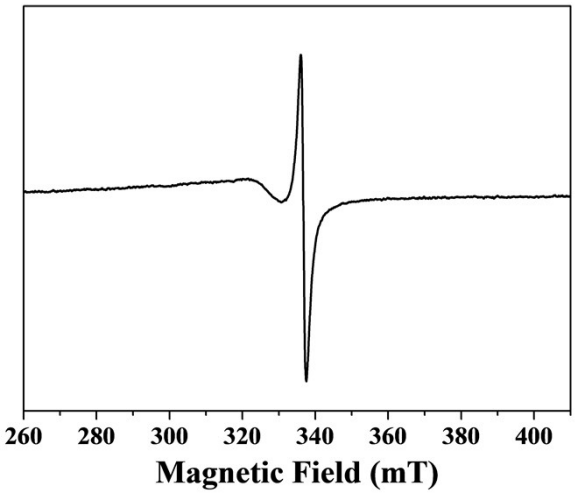

Figure S5. ESR spectrum of VCR-PEG-CuPani NSs.

Table S2. The mass fraction of various elements in CuPani and PEG-CuPani, which exhibits the increase in H, O, Fe, Cu and decrease in C, N.

Mass Precent	C(%)	H(%)	N(%)	O(%)	Fe(%)	Cu(%)	Cl(%)
CuPani	32.81	2.49	6.38	1.68	11.49	11.01	34.14
PEG-CuPani	29.72	2.86	4.61	3.05	12.18	11.69	35.89

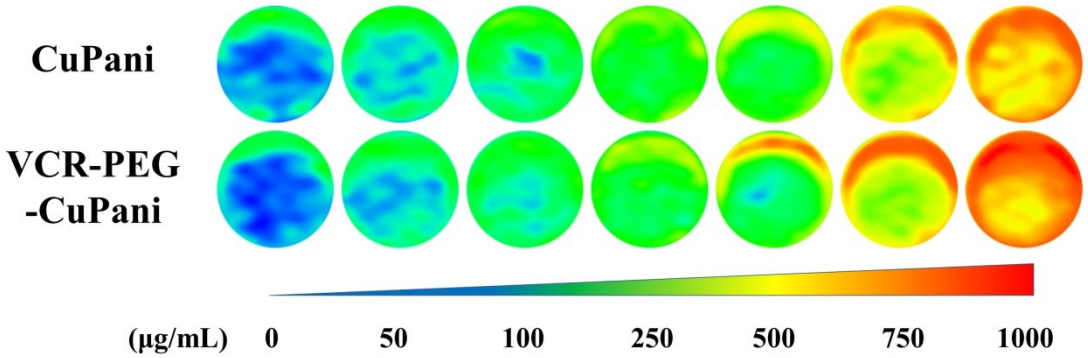

Figure S6. Concentration-dependent T_1-weighted MRI of CuPani NSs (a) and VCR-PEG-CuPani NSs (b) under a 1.5 T magnetic field. The color bar from blue to red represents the MRI signal from low to high.

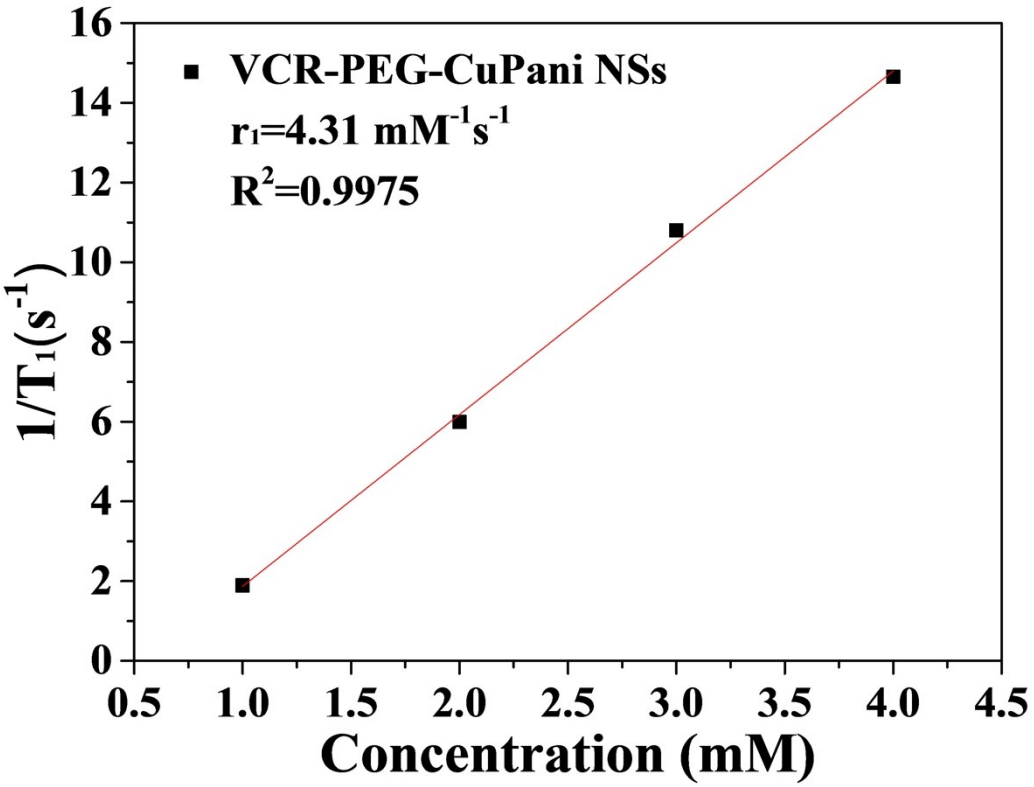

Figure S7. Longitudinal relaxation rate (r_1) for VCR-PEG-CuPani NSs.

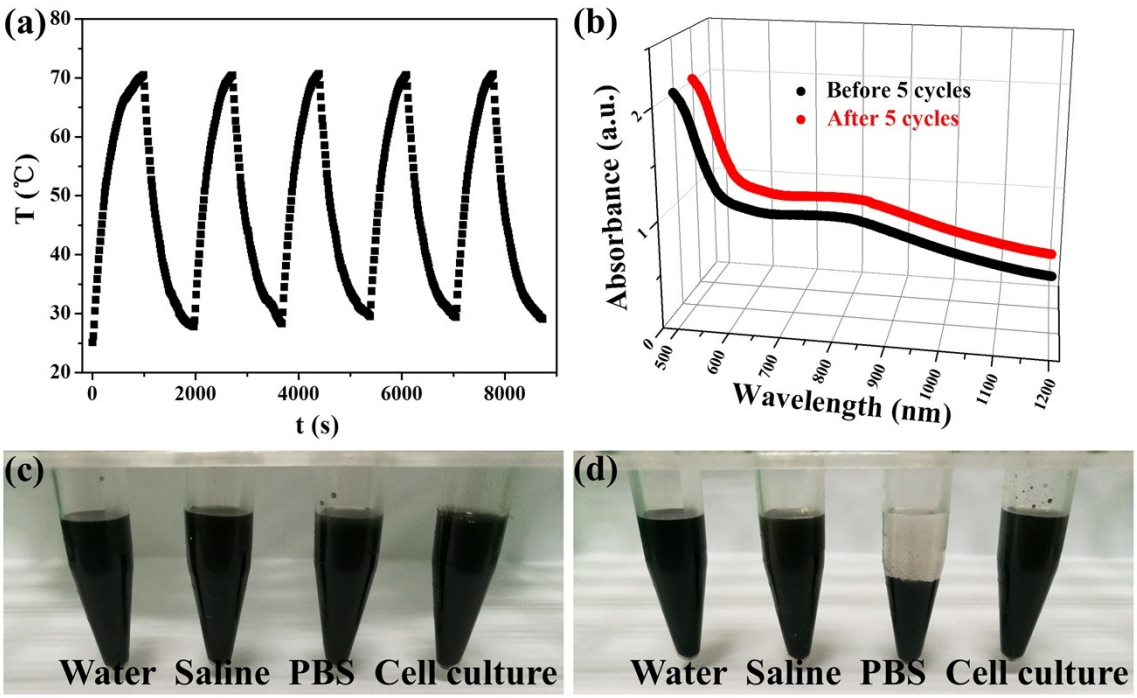

Figure S8. (a) The real-time temperature records of VCR-PEG-CuPani NSs solution as heating up and cooling down for 5 cycles at the time interval of 15 s. The laser power density is 3.5 W/cm^2, and the concentration of VCR-PEG-CuPani NSs is 50 μg/mL. (b) The UV-vis-NIR absorption spectra of VCR-PEG-CuPani NSs solution before and after 5 cycles. (c) Photographs of VCR-PEG-CuPani NSs solution in pure water, saline, PBS and cell culture medium. (d) Photographs of VCR-PEG-CuPani NSs solution in pure water, saline, PBS and cell culture medium after 2 weeks incubation and gently shake.

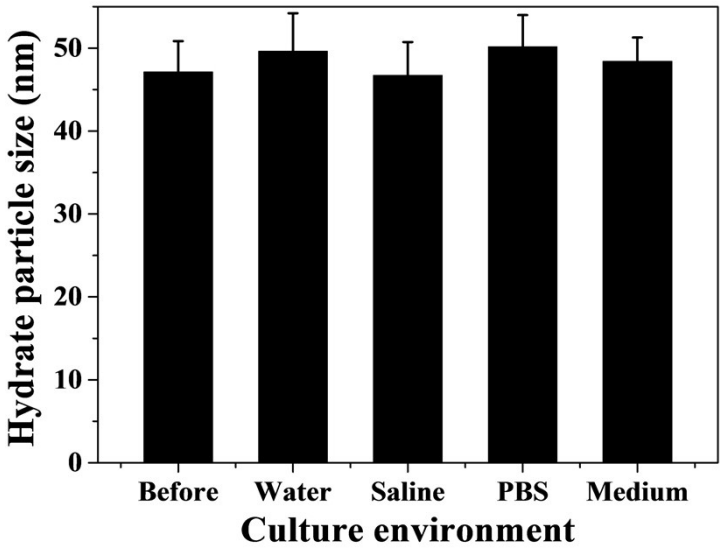

Figure S9. Comparison of the hydrate size distribution of the VCR-PEG-CuPani NSs before and after 2 weeks incubation in pure water, saline, PBS and cell culture medium by dynamic light scattering. The size of VCR-PEG-CuPani NSs has no significant change.

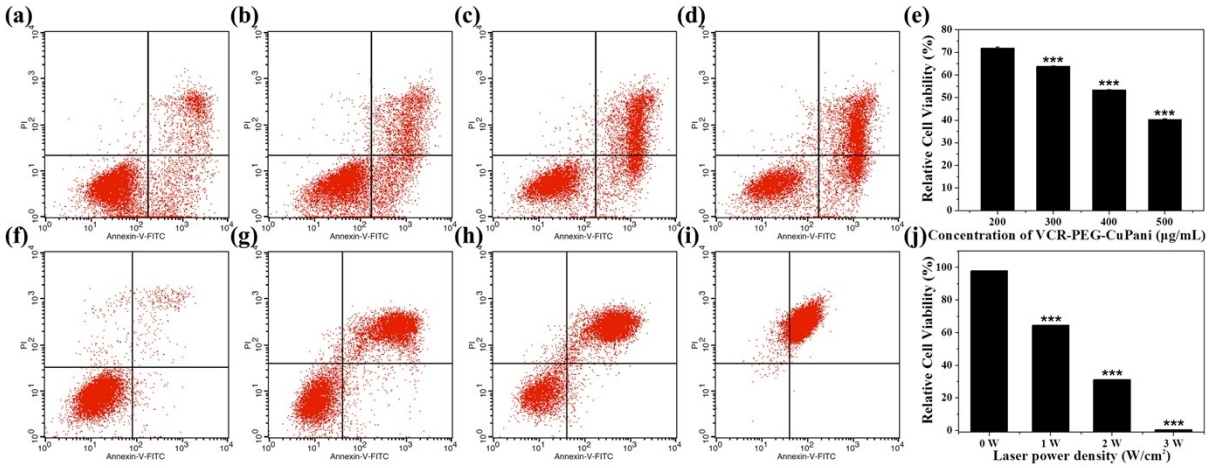

Figure S10. KB cells are incubated with different concentration of VCR-PEG-CuPani NSs at 200 (a), 300 (b), 400 (c) and 500 (d) μg/mL for 24 h, and the cell viabilities are estimated through flow cytometry analysis. Percentages of living cells: (a) 72.0 ± 0.4 %, (b) 63.9 ± 0.2 %, (c) 53.4 ± 0.2 %, (d) 40.3 ± 0.3 %. (e) Histogram and statistical analysis of cell viability in (a)-(d). KB cells are incubated with 50 μg/mL VCR-PEG-CuPani NSs for 1 h, and then irradiated by an 808 nm laser at the power density of 0 (f), 1 (g), 2 (h) and 3 (i) W/cm^2 for 10 min. The cell viabilities are estimated through flow cytometry analysis. Percentage of living cells: (f) 97.9 ± 0.1 %, (g) 64.6 ± 0.2 %, (h) 31.1 ± 0.3 %, (i) 0.4 ± 0.1 %. (j) Histogram and statistical analysis of cell viability in (f)-(i). Data are shown as the means ± standard error of the means, with *** $p < 0.001$.

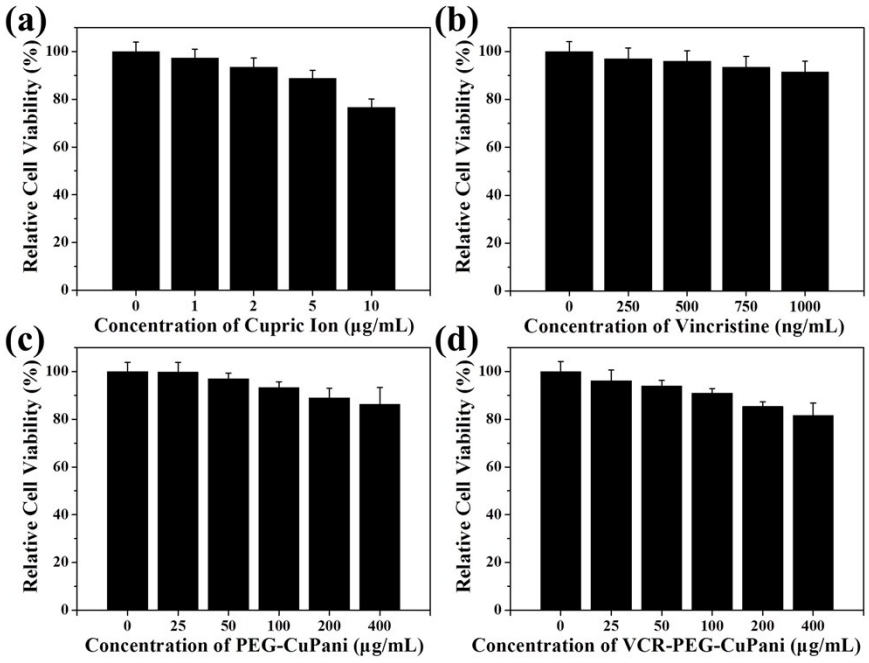

Figure S11. HaCat cells are incubated with different concentrations of cupric ions (a), vincristine (b), PEG-CuPani NSs (c) and VCR-PEG-CuPani NSs (d) for 24 h, and then the cell viabilities are estimated through standard CCK-8 assay.

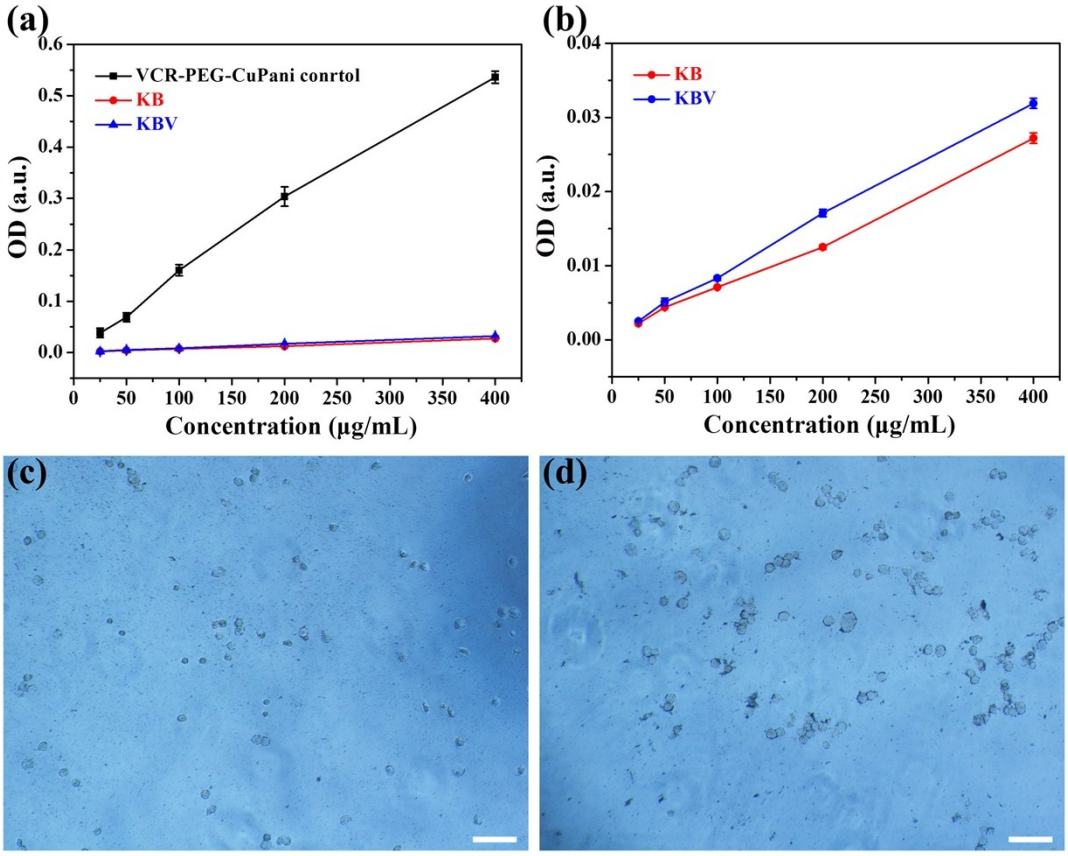

Figure S12. Nonspecific cellular adhesion of VCR-PEG-CuPani NSs. (a) KB and KBV cells are incubated with different concentrations of VCR-PEG-CuPani NSs at 25, 50, 100, 200 and 400 μg/mL, the amounts of nanomaterials adhered to cell surface are estimated through measuring the OD values. The VCR-PEG-CuPani control represents the OD values at different concentrations. (b) A partially enlarged image of Figure (a) for a more intuitive observation. The photographs of VCR-PEG-CuPani NSs adhered to KB (c) and KBV (d) cells at the concentration of 100 μg/mL. The scale bar is 50 μm.

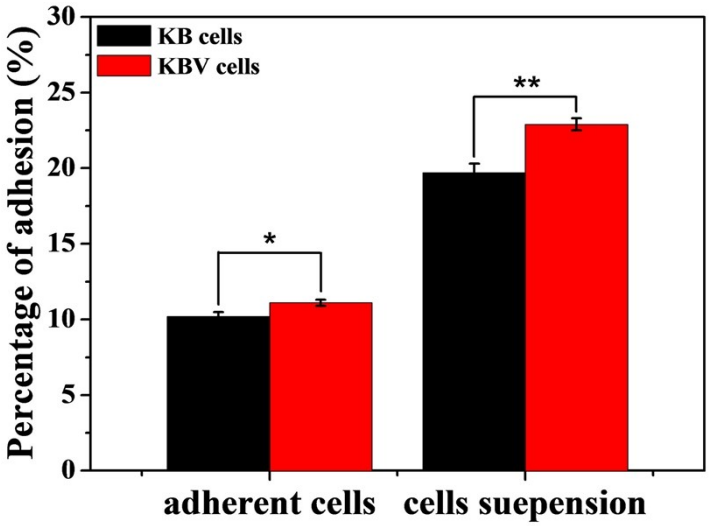

Figure S13. Experimental results of cell adhesion of nanomaterials. For adherent cells, the cell adhesion/uptake rate for KB and KBV cells is 10.2±0.3 % and 11.1±0.2 %, respectively. In the cell suspension, the cell adhesion/uptake rate for KB and KBV cells is 19.7±0.6 % and 22.9±0.4 %, respectively. Data are shown as the means ± standard error of the means, with * $p < 0.05$, and ** $p < 0.01$.

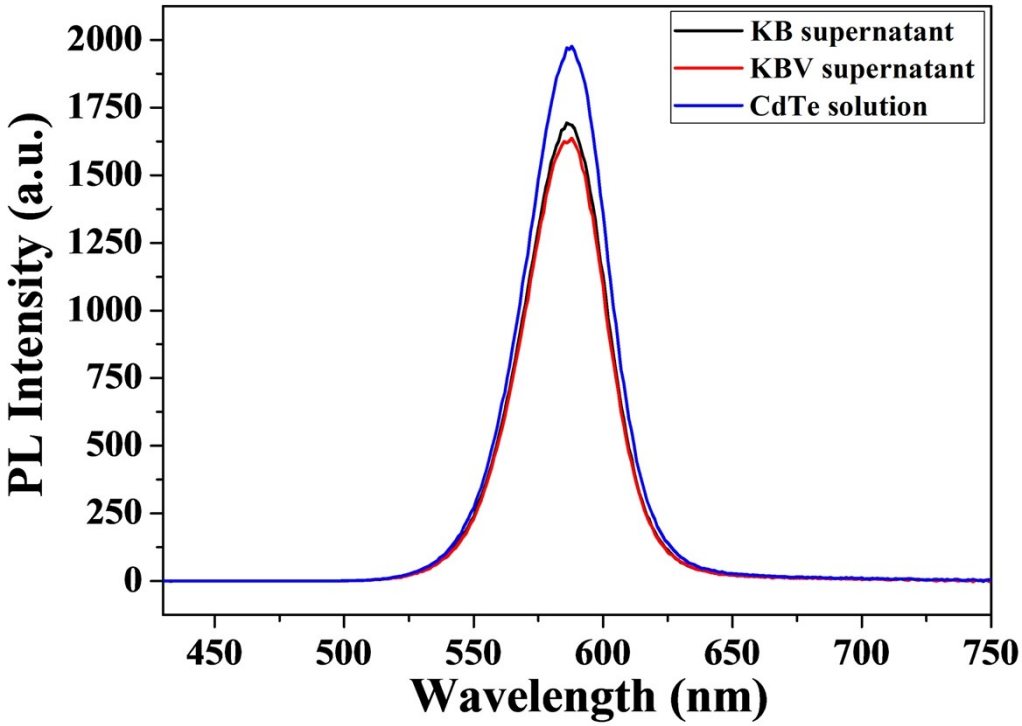

Figure S14. The same amount of positive charged CdTe quantum dots is mixed with the same number of KB and KBV cells, respectively. One hour later, the two groups of mixture are centrifuged at 2000 r/min for 5 minutes to remove the cells adhered with quantum dots. The intensity of the photoluminescence emission of the supernatants is compared. The emission intensity of the supernatant of KB cell group is higher, which means that the amount of quantum dots adhered on KB cells is less.

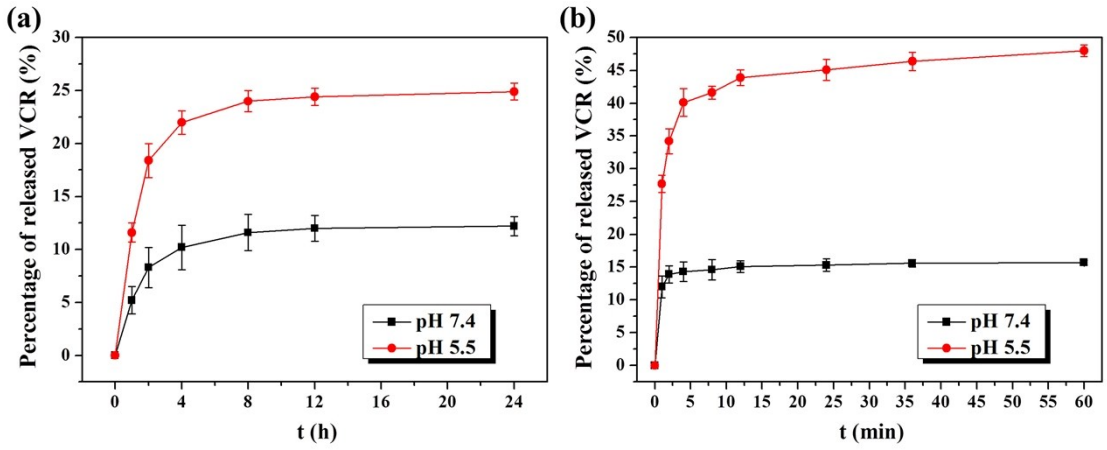

Figure S15. Drug release curves of VCR under different pH environment without (a) or with (b) laser treatment.

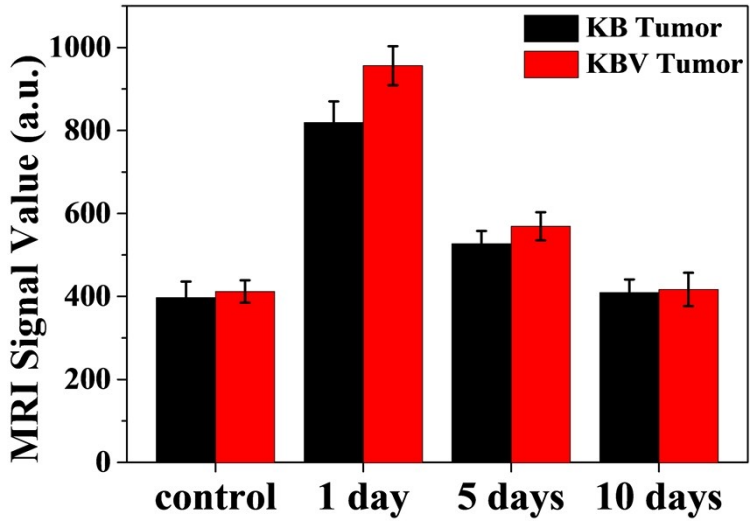

Figure S16. MRI signal values of KB and KBV tumors in different time point.

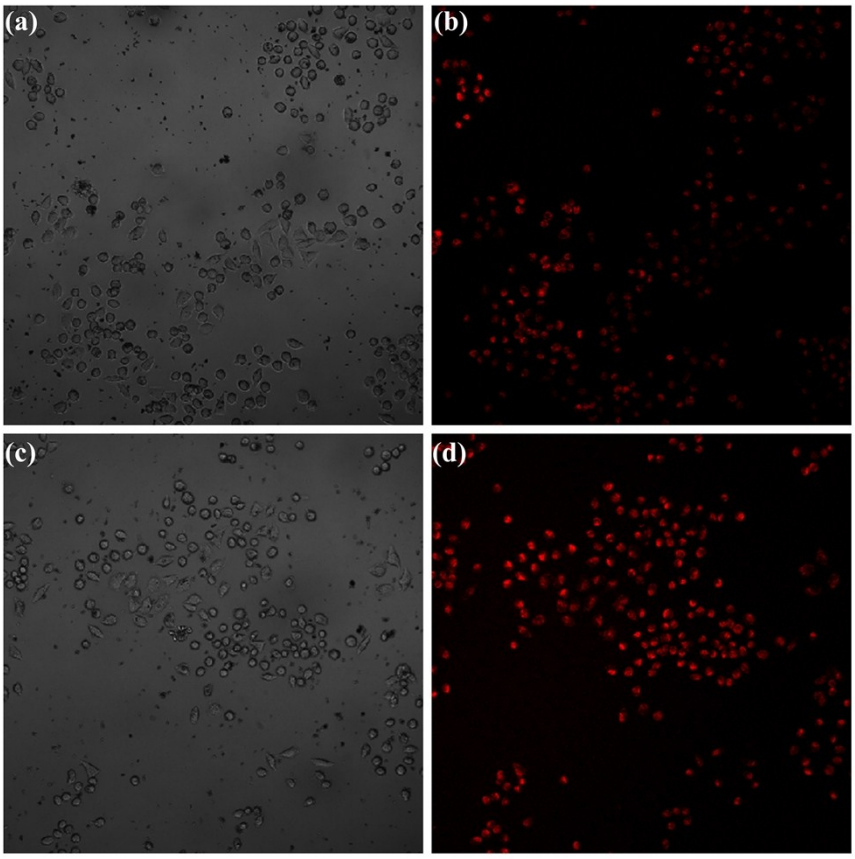

Figure S17. KB and KBV cells are incubated with red-fluorescent-labeled VCR-PEG-CuPani NSs at 50 μg/mL for 24 h, and the images are obtained through laser scanning confocal microscope. The dark field photograph (a) and fluorescent photograph (b) of KB cells. The dark field photograph (c) and fluorescent photograph (d) of KBV cells.

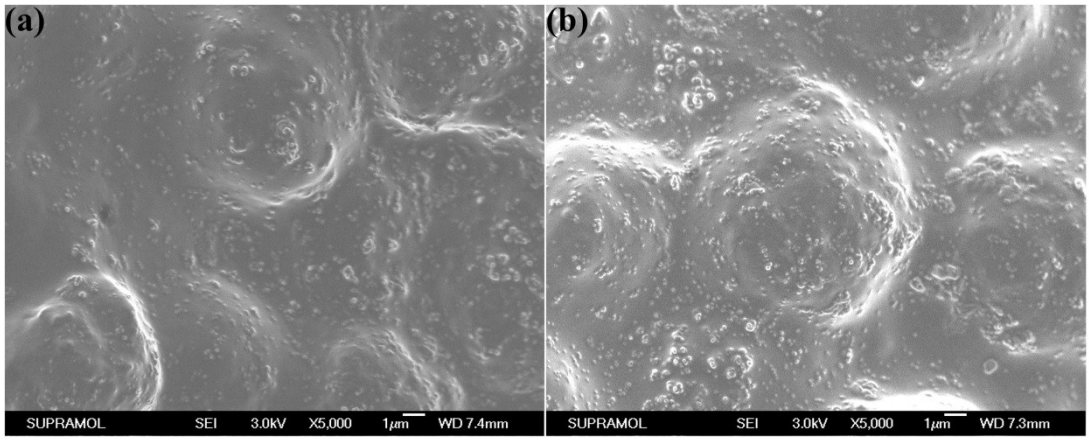

Figure S18. SEM images of KB (a) and KBV (b) cell surface structure, which shows a difference in the amount of protein on the surface of the cell membrane.